PHYSICAL REVIEW B VOLUME 42, NUMBER 16 1 DECEMBER 1990

Flux-flow Hall-effect problem: Comparison of the theory of Nozières and Vinen with results in $2H$-$NbSe_2$

T. W. Jing and N. P. Ong
Joseph Henry Laboratories of Physics, Princeton University, Princeton, New Jersey 08544
(Received 19 July 1990)

The old problem of the flux-flow Hall effect is investigated in single-crystal $2H$-$NbSe_2$. We find that the Hall signal, particularly the constancy of the Hall angle with field, is correctly described by the theory of Nozières and Vinen (NV). The dependences of θ_H on field, current density, and temperature are compared in some detail with the version of NV's model that assumes a finite pinning force.

The Hall effect due to vortex motion in type-II superconductor is a venerable, and perplexing, problem that has been of interest for 26 yrs.[1-6] In principle, the Hall voltage V_H should provide a more sensitive test of models for vortex motion than the resistivity alone. Although V_H has been measured in many conventional superconductors and, recently, in the oxide superconductors,[7] published experimental results show little, if any, resemblance to theoretical predictions. In the model of Bardeen and Stephen (BS),[2] the Hall angle θ_H is given by $\tan\theta_H = \omega_c\tau$, where $\omega_c = eB/m$, e and m are the electronic charge and mass, and τ is the relaxation time in the normal core. Nozières and Vinen (NV)[3] predict, however, that θ_H remains constant below the upper critical field H_{c2}, viz.,

$$\tan\theta_H = \beta \equiv eH_{c2}\tau/m . \quad (1)$$

Measurements[4,5] on alloys such as Nb-Ta and Ti-Mo with l/ξ as small[5] as 10^{-2} (extreme dirty limit) show that $\tan\theta_H$ is much larger than predicted by either theory (l is the mean free path and ξ the coherence length). In single-crystal Nb, the measured $\tan\theta_H$ falls below the BS prediction.[1,2] The constant behavior of θ_H predicted by Eq. (1) has never been observed. The situation has been further confused by findings that $\tan\theta_H$ is strongly influenced by macroscopic defects. For instance, linear defects introduced by rolling lead to "guided motion" of the vortex lines.[4,6] Part of the difficulty is that most experiments [except those on Nb (Ref. 1)] are performed on superconductors in the *dirty* limit, whereas the models apply only to the clean limit.

To investigate the problem anew, we have chosen the anisotropic superconductor[8-14] $2H$-$NbSe_2$, which is easily grown in high-purity single-crystal form free of macroscopic inhomogeneities. In our samples the average l (estimated[12] from the Hall effect[10] and band structure[11]) is ~480 Å at 8 K, corresponding to $l/\xi_{ab} = 6.2$ (ξ_{ab}, the coherence length in the basal plane[8] ≈ 77 Å). The crystals can be cleaved to a thickness of 30 μm, which facilitates the application of large current densities J. The large H_{c2} (~4.4 T at 1.06 K) (Ref. 8) also allows the use of intense fields, so that the flux-flow regime may be reached with modest J. All our samples have the same nominal T_c (7.2 K at zero field) and H_{c2} vs T profile.

Figure 1 (main panel) displays the variation with H of the longitudinal and Hall resistivities, ρ_{xx} and ρ_{xy}, respectively, in sample 1 at 4.2 K. In the field range 0.7–1.8 T, both ρ_{xx} and ρ_{xy} increase linearly with the field. A sharp minimum is observed in ρ_{xx} (the "peak" effect) (Ref. 13) just below $H_{c2} \sim 2.05$ T (defined as where ρ_{xx} rises steeply). Below ~0.7 T, ρ_{xx} lies above the straight line drawn through the linear portion at higher fields. This "excess voltage" is due to activated flux motion (V_H is very weak in this activated regime). Our interest lies in the linear regime at higher fields, that we identify with coherent flux motion. Above H_{c2}, ρ_{xx} rises slowly to its normal-state value ρ_N, instead of abruptly. The inset, displaying the pinning force density versus field, is discussed later.

To test Eq. (1), we plot in Fig. 2 the field dependence of $\rho_{xy}/\rho_{xx} = \tan\theta_H$ in sample 1 (at 4.2 K) and sample 2 (at 5.5 K). In both cases, $\tan\theta_H$ increases steeply as soon as H exceeds a threshold field, and then assumes a constant value until interrupted by the peak effect. (In the normal state, $H > H_{c2}$, $\tan\theta_H$ increases linearly with H.) Thus, unlike in previous experiments, a plateau in $\tan\theta_H$ is clearly observed over a wide range of fields below H_{c2}, as

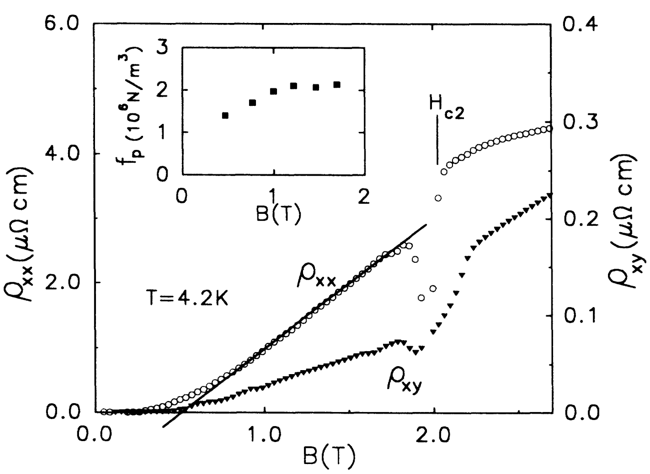

FIG. 1. (Main panel) The field dependence of ρ_{xx} (open symbols) and ρ_{xy} (solid symbols) in $2H$-$NbSe_2$ (sample 1) at 4.2 K, taken with $J = 553$ A/cm^2. Both ρ_{xy} and ρ_{xx} increase linearly with the reduced field $H - H_p$ (straight line). The inset shows the field variation of f_p in sample 1 at 4.2 K, determined from E_x vs J curves. Contacts (~1 mΩ) are attached with In solder. (H is applied normal to the basal plane.)

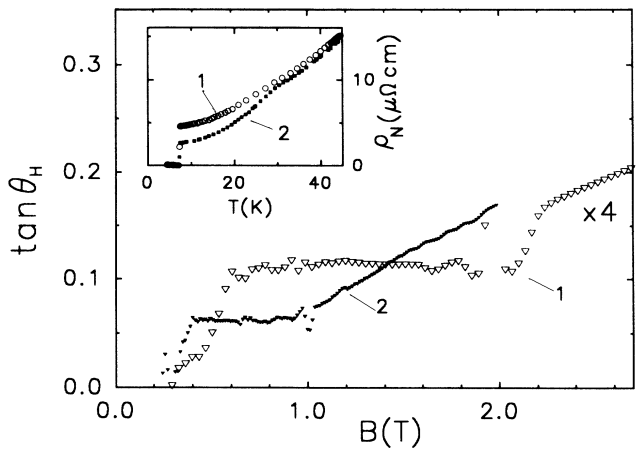

FIG. 2. (Main panel) The variation of $\tan\theta_H$ with field in sample 1 (open symbols, at 4.2 K) and in sample 2 (solid symbols, at 5.5 K), showing the constant value below H_{c2}. (At these temperatures, H_{c2} is 2.05 and 1.0 T, respectively.) The inset shows ρ_N vs T in the two samples. Sample 2 (solid squares) has a larger conductivity and Hall angle below the CDW transition at 32 K.

predicted by NV. The magnitude of $\tan\theta_H$ is more subtle. From Fig. 2, $\tan\theta_H$ is clearly dependent on both the temperature and the value of ρ_N, i.e., l, in each sample.

In 2*H*-NbSe$_2$, the charge-density wave transition[14] near 32 K alters the Fermi surface (FS), and drives ρ_{xy} negative.[10] Interestingly, this substantially enhances the conductivity (and l) in some samples (our sample 2), while in others (1 and 3), ρ_N is barely affected (Fig. 2, inset). Within experimental error, ρ_N is the same in the three samples between 290 and 32 K, but it is 40% smaller in sample 2 at 8 K. The normal-state Hall angle in sample 2 also exceeds that in samples 1 and 3 by a large factor ($\sim$4.2), indicating the existence of a small FS pocket[15] with a very long l in sample 2. The large difference in the normal-state Hall angle, previously unreported, does not affect the superconducting parameters, but changes the flux-flow Hall angle by a factor of $\sim$4.4 (compared at the same T). However, regardless of the differences due to different T's and l's, the value of $\tan\theta_H$ at the plateau in each sample is nominally equal to the value of $\omega_c\tau$ at the field $H_{c2}(T)$ (we return to this below). To compare with the theory further, we need to discuss the effects of pinning, and the current dependence of ρ_{xx} and ρ_{xy}.

Since Hall measurements are performed by either sweeping J or H, one proceeds from the pinned regime, and (at large J or H) approaches the free-flow regime, without quite attaining it. Thus, the Hall experiments are always executed in a regime in which the pinning force $\mathbf{F}_p$ *cannot* be neglected. We next summarize the salient features of the version of NV's model[3] that incorporates a finite $\mathbf{F}_p$. Because $\mathbf{F}_p$ retards the vortex line velocity $\mathbf{v}_L$, the drift velocity of the normal electrons in the core $\mathbf{v}_{nc}$ lags the applied supercurrent velocity $\mathbf{v}_{s1}$ by $\Delta\mathbf{v}_c \equiv \mathbf{v}_{s1} - \mathbf{v}_{nc}$ ($\mathbf{v}_{s1} \equiv \mathbf{J}/ne$, where n is the superfluid density). NV assume that $\mathbf{F}_p$ is proportional to $\Delta\mathbf{v}_c$, and perpendicular to it, viz.,

$$\mathbf{F}_p = -ne\Delta\mathbf{v}_c \times \boldsymbol{\phi} \tag{2}$$

(where $\phi = h/2e$ and $\boldsymbol{\phi} = \mathbf{B}\phi/B$). The total Magnus force $\mathbf{F}_{\rm Mag} = ne(\mathbf{v}_{s1} - \mathbf{v}_L) \times \boldsymbol{\phi}$ acting on a unit length of the vortex (core plus transition layer) may be divided into two components, $\mathbf{F}_{\rm bulk}$ (acting on the bulk of the core) and $\mathbf{F}_{\rm conv}$ (on the transition layer). The former is given by $\mathbf{F}_{\rm bulk} = (ne/2)\ (\mathbf{v}_{s1} - \mathbf{v}_L) \times \boldsymbol{\phi} + (ne/2)\Delta\mathbf{v}_c \times \boldsymbol{\phi}$. Balancing $\mathbf{F}_{\rm bulk}$ and $\mathbf{F}_p$ against the rate of momentum relaxation inside the core, NV obtain the equation of motion

$$\mathbf{F}_{\rm bulk} + \mathbf{F}_p = n\pi\xi^2 m\mathbf{v}_{nc}/\tau = (ne\phi/2\beta)\mathbf{v}_{nc}\,. \tag{3}$$

With the additional assumption that $\mathbf{v}_{nc} \| \mathbf{v}_{s1}$, the solution for $\mathbf{v}_L$ for an *isolated* vortex is [9]

$$\mathbf{v}_L = (v_{s1} - \Delta v_c)[\hat{\mathbf{x}} + \hat{\mathbf{y}}/\beta]\,. \tag{4}$$

Here, $\Delta v_c = F_p/ne\phi$, and we take $\mathbf{J} \| \hat{\mathbf{x}}$ and $\mathbf{H} \| -\hat{\mathbf{z}}$. In the flux-flow state, the ratio of the electric fields E_y/E_x ($\tan\theta_H$) equals v_{Lx}/v_{Ly}, which is just the constant β, by Eq. (4). Thus, NV obtain the remarkable result that a finite pinning force does not affect the flux-flow Hall angle in the clean limit. This ensures that Eq. (1) applies over a *finite* range of fields below H_{c2}, i.e., throughout the coherent flow regime, instead of just predicting a limiting value.

To describe the collective motion of the flux lattice, we consider a vortex bundle of linear size L undergoing rigid (coherent) motion.[9] NV's model is easily generalized to describe the motion, provided $\mathbf{F}_p$ is scaled properly. In place of F_p in Eq. (4), we substitute the pinning force *density* $f_p = L^{-2}|\sum_i \mathbf{F}_p^i|$, where the sum is restricted to the pins i in the bundle. Eliminating $\mathbf{v}_L$ and $\mathbf{v}_{s1}$ in favor of $\mathbf{E}$ and $\mathbf{J}$, respectively, we get for the bundle[9]

$$E_x = (BJ - f_p)/ne\beta,\ E_y = E_x\beta\,. \tag{5}$$

Equation (5) predicts that $\rho_{xx} = E_x/J$ is zero until H exceeds a pinning field $H_p \equiv f_p/J$. Thereafter, it increases linearly with the reduced field $(H - H_p)$, with a slope $d\rho_{xx}/dH$ equal to that in the free case,[16] provided f_p is independent of H. By Eq. (5), E_y increases *linearly* with $(H - H_p)$ as well.[16] Equation (5) is also quite specific about the J dependences. Whereas both ρ_{xy} and ρ_{xx} scale linearly with the reduced current $(J - J_p)$, their ratio, $\tan\theta_H$, is *independent* of J (provided JB exceeds f_p).

We now compare Eq. (5) in some detail with our results. In Fig. 1, the solid lines indicate that, in the range 1.0–1.8 T, both ρ_{xx} and ρ_{xy} increase linearly with the reduced field, consistent with Eq. (5). By extrapolating the straight lines to the field axis, the pinning field H_p is seen to be equal to 0.50 T for both ρ_{xx} and ρ_{xy}. The observed linear behavior implies that f_p is not strongly field dependent. This can be checked by examining the E_x vs J curves at this T in different fields. Direct measurement[9] of E_x vs J show that at large J, E_x increases linearly with the reduced current $(J - J_p)$, in agreement with Eq. (5). At low J, however, E_x lies significantly above the extrapolated straight line. This is the activated contribution mentioned above. By extrapolating the linear segment to the J axis, we have determined the "depinning" current density J_p at each value of H, and computed the pinning force density $f_p = J_pH$, which is plotted in the inset of Fig. 1. For the field range, 1.0–1.8 T, in which coherent flux flow occurs, we find that f_p is indeed only weakly dependent on

H. (Below 1 T, f_p falls with decreasing H. In this field regime, we are less confident of the determination of f_p from extrapolation of the linear behavior since the activated processes dominate ρ_{xx}.)

The current dependence may also be examined by plotting ρ_{xx} and $\tan\theta_H$ vs H at two values of J (Fig. 3). As mentioned above, Eq. (5) predicts that the slope of ρ_{xx} vs H in the linear regime should be independent of J, but the pinning field H_p should scale as $1/J$. This is consistent with the data, which show that, in the linear regime, the two ρ_{xx} vs H curves are parallel. The respective H_p's also match the inverse ratio of the J's, to the accuracy of the measurement. Equation (5) also predicts that, at the plateau, $\tan\theta_H$ should be independent of J, except for the difference in threshold fields. Within experimental error, this is also borne out in the data. Closer examination shows that the lower J data consistently lie $\sim 10\%$ above the higher J data. This difference may arise from slight heating of the sample at the larger J (H_{c2} is slightly depressed by 0.17 T).

Last, we consider the temperature dependence. As T approaches the transition $T_c = 7.2$ K, both the superfluid density n_s and H_{c2} decrease linearly with $(1-t)$, where $t \equiv T/T_c$. How is Eq. (1) affected by these changes? NV's model is formulated at $T=0$, and it is not clear how Eqs. (1)-(4) are changed when n_s falls below its value at $T=0$. All our measurements are at fairly high reduced temperatures ($t=0.58$ and 0.76), but, within the uncertainty of our measurements, we do not observe any finite temperature corrections to Eqs. (1) and (4) (apart from that in β, through H_{c2}). For example, we compare in Fig. 4, $\tan\theta_H$ at two temperatures in sample 3. At the plateau, the ratio of $\tan\theta_H$ at 4.2 and 5.5 K is found to match the ratio of the H_{c2}'s. We note further that the ratio of the slopes $d\rho_{xx}/dH$ at the two T's (in the linear regime) also scales with H_{c2}, in good agreement with Eq. (5). Thus, Eqs. (1) and (5) apply at both T, i.e., *all the T dependence arises from β*, through H_{c2}. [Hence, n is independent of T in Eq. (5)]. This implies that, in the generalization of Eq. (3) to finite T, $n_s(T)$ should be used for n in *both* expressions for $\mathbf{F}_{\mathrm{bulk}}$ and the $\mathbf{v}_{nc}$ (core) term. This is surprising to us since all the core electrons should be involved in the momentum relaxation. A related problem is the large variation of $\tan\theta_H$ between high-mobility and low-mobility samples. In Fig. 2, the ratio of $\tan\theta_H$ between samples 2 and 1 (4.4) is much closer to their Hall angle ratio (4.2) than their conductivity ratio (1.7). The latter would have been the obvious choice, since dissipation within the core is involved. A generalization of NV's theory to finite temperatures in a multiband system would be helpful.

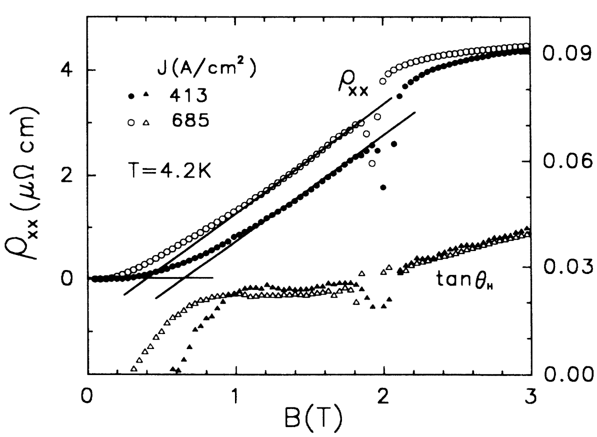

FIG. 3. Comparison of ρ_{xx} and $\tan\theta_H$ in sample 3 taken at two different J's (685 and 413 A/cm^2). At the larger J (open symbols) ρ_{xx} has a smaller threshold field H_p (the intercept of the straight line with the H axis). However, the two curves are parallel in agreement with Eq. (5). Within our accuracy, the values of $\tan\theta_H$ are also equal for the two J's, except near threshold.

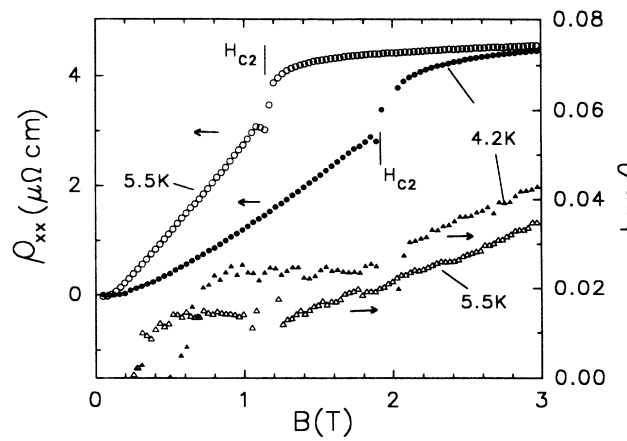

FIG. 4. Comparison of ρ_{xx} and $\tan\theta_H$ in sample 3 taken at 4.2 and 5.5 K, the same J (685 A/cm^2). At 5.5 K (open symbols), ρ_{xx} has a steeper slope and $\tan\theta_H$ is smaller. The ratio of $\tan\theta_H$ at the plateau ($0.024/0.014 = 1.71$) agrees with the ratio of H_{c2}'s ($1.92/1.13 = 1.70$). The ratio of the slopes $d\rho_{xx}/dH$ in the linear regime equals 1.73.

In summary, we have shown that, contrary to previous experiments,[1,4-6] the model of Nozières and Vinen[3] with finite $\mathbf{F}_p$ provides the correct description of the flux-flow Hall and longitudinal resistivities for a type-II superconductor in the clean limit. Equation (5) accurately predicts the field and current dependences of ρ_{xx} and ρ_{xy}. Empirically, finite-temperature effects are accurately described if n is replaced in Eq. (3) by $n_s(T)$ [but n is T independent in Eq. (5)]. This remains to be justified theoretically. The good agreement supports the validity of the assumptions NV made regarding the nature of $\mathbf{F}_p$, and on the orientation of $\mathbf{v}_{nc}$ relative to $\mathbf{v}_{s1}$. This precludes the need for introducing additional damping forces in this problem. The two Hall features, linearity of ρ_{xy} vs $H - H_p$, and constancy of θ_H, may be taken as characteristic signatures of the coherent flow state. (These two features remain unchanged as J or H is increased further, except at the peak effect.) Further studies of the temperature dependence in $2H$-NbSe$_2$, as well as in other systems, in single-crystal form, with large H_{c2} and ξ/l are desirable. Given the sensitivity of the Hall signal to macroscopic inhomogeneities,[4,6] tests carried out in thin-film, amorphous, or polycrystalline samples are unreliable, because such inhomogeneities therein are harder to eliminate.

This research is supported by the Office of Naval Research Contract No. N00014-90-J-1013 and by a Grant from the Seaver Foundation.

---

[1]W. A. Reed, E. Fawcett, and Y. B. Kim, Phys. Rev. Lett. **14**, 790 (1964).

[2]J. Bardeen and M. J. Stephen, Phys. Rev. **140**, A1197 (1965).

[3]P. Nozières and W. F. Vinen, Philos. Mag. **14**, 667 (1966).

[4]A. K. Niessen, F. A. Staas, and C. H. Weijsenfeld, Phys. Lett. **25A**, 33 (1967); C. H. Weijsenfeld, *ibid.* **28A**, 362 (1968).

[5]R. R. Hake, Phys. Rev. **168**, 442 (1968).

[6]F. A. Staas, A. K. Niessen, W. F. Druyvesteyn, and J. V. Suchtelen, Phys. Lett. **13**, 293 (1964).

[7]Y. Iye, S. Nakamura, and T. Tamegai, Physica C **159**, 433 (1989); **159**, 616 (1989); T. R. Chien, Z. Z. Wang, and N. P. Ong (unpublished). In $YBa_2Cu_3O_7$, ρ_{xy}/ρ_{xx} measured between 73 and 92 K cannot be identified with $\tan\theta_H$ because ρ_{xy} and ρ_{xx} have very different threshold fields.

[8]P. de Trey, Suso Gygax, and J. P. Jan, J. Low Temp. Phys. **11**, 421 (1973). From this work, the coherence lengths are $\xi_{ab}=77$ Å, $\xi_c=23$ Å. The ratio $\xi_{ab}/\xi_c=3.4$ is to be compared with ~5 estimated for $YBa_2Cu_3O_7$.

[9]T. W. Jing and N. P. Ong (unpublished).

[10]H. N. S. Lee, H. McKenzie, D. S. Tannhauser, and A. Wold, J. Appl. Phys. **40**, 602 (1969).

[11]L. F. Mattheiss, Phys. Rev. B **8**, 3719 (1973).

[12]Above 60 K, the Hall effect has been shown to agree well with the band structure in Ref. 10. Fits to ρ_{xy} and ρ_{xx} using a multiband model yield the *areal* densities (per Nb-Se layer) $n_1=2.2\times10^{14}$ cm^{-2} and $n_2=4.1\times10^{14}$ cm^{-2}, and the mean free paths $l_1=6.2$ Å, $l_2=8.8$ Å at 350 K for the two distinct Fermi surface pockets. To estimate an *average* l at 8 K, we multiplied the numbers at 350 K by the residual resistivity ratio (30 and 54 in samples 1 and 2, respectively). N. P. Ong, Phys. Rev. B (to be published).

[13]K. E. Osborne and E. J. Kramer, Philos. Mag. **29**, 685 (1974).

[14]J. A. Wilson, F. J. DiSalvo, and S. Mahajan, Adv. Phys. **24**, 117 (1975).

[15]The much larger enhancement of θ_H in sample 2 (4.4 times that in 1) compared with the enhancement in conductivity (1.7 times) suggests the existence of a small FS pocket with a long l. Such a pocket is observed in magnetothermal oscillation experiments. See John E. Graebner and M. Robbins, Phys. Rev. Lett. **36**, 422 (1976).

[16]If $f_p=0$, Eq. (5) recovers the Bardeen-Stephen law (Ref. 2) $[\rho_{xx}=(H/H_{c2})\rho_N]$. Note that when $f_p=0$, $E_y\sim H$ in the NV model, but $E_y\sim H^2$ in the BS model.